Self-association Mechanisms in Aqueous Media: Dimerization *versus* Micellization of Alkyl-ellipticinium Derivatives

Alain Adenier,* Marie-Anne Cordonnier, Marie-Françoise Ruasse and Marc-Antoine Schwaller
Institut de Topologie et de Dynamique des Systèmes de l'Université Paris 7, associé au CNRS URA 34, 1 rue Guy de La Brosse, 75005 Paris, France

Self-association mechanisms in aqueous media of ellipticinium (E), 2-methylellipticinium (2-NME), oxazolopyridocarbazolium (H-OPC), 10-pentyloxazolopyridocarbazolium (10-pentyl-OPC), 2 aminopentyloxazolopyridocarbazolium (2-aminopentyl-OPC) and 2-pentyloxazolopyridocarbazolium (2-pentyl-OPC) acetates have been investigated by spectroscopic and kinetic studies. Whereas E, 2-NME, H-OPC, 10-N-pentyl-OPC and 2-aminopentyl-OPC dimerize by self-stacking, the 2-pentyl-OPC displays micellar behaviour (with a critical micellar concentration of 20 μmol dm^{-3}), as a direct consequence of its amphiphilic character. As regards dimerization, both aliphatic substitution (K_d = 7.6 × 10^3 and 2.4 × 10^4 dm^3 mol^{-1} for E and 2-NME, respectively) and extension of the π-electron aromatic system (K_d = 1.4 × 10^5 and 4.5 × 10^5 dm^3 mol^{-1} for H-OPC and 10-pentyl-OPC, respectively) significantly increase the dimer stability. From kinetic analysis, dimer stability seems to be controlled mainly by the reverse rate constants which vary from 4.9 × 10^4 to 1.9 × 10^3 s^{-1}.

The plant alkaloid ellipticine (5,11-dimethyl-6*H*-pyrido[3,4-*b*]carbazole, **1a**) and some of its quaternarized derivatives (**1b**)

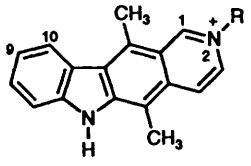

1a, R = H:
1b, R = Me.

are used as antitumour agents in the treatment of various human cancers.[1] *In vivo*, these molecules are bioactivated *via* oxidation and coupling with biological nucleophiles, leading to a new extended polycyclic, 7,10,12-trimethyl-6*H*-oxazolo[4,5-*a*]pyrido[4,3-*i*]carbazolium acetate (H-OPC), **2a**. As do many

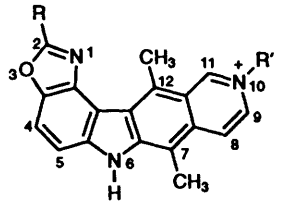

2a, R = H; R′ = CH_3
2b, R = $CH_3(CH_2)_4$–; R′ = CH_3
2c, R = H; R′ = $CH_3(CH_2)_4$
2d. R = $NH_3^+(CH_2)_5$–; R′ = CH_3

planar aromatic cations, these molecules bind strongly to DNA by intercalation,[2] a process arising from stacking interactions between the chromophoric drug and the DNA bases.[3] Another direct consequence of their molecular structure is their self-association in aqueous solution.[4] The most simple self-association mechanism involves dimerization according to an intermolecular stacking process involving mainly London-type dispersion interactions[5] between the chromophoric groups. It has been shown previously in the alkyl acridine orange (AO) series[6] that additional hydrophobic chain–chain interactions increase the dimer stability. In the case of the ellipticine series, we have found previously[7] that, in addition to the classical dimerization process, micellization can occur when the aliphatic chain in the C-2 position of **2a** consists of at least four methylene units. We report now results on the influence of the relative position of the aliphatic chain and the quaternary ammonium group on the self-association mechanism. In particular, comparison of the aggregation modes of **2b** and **2c** where the aliphatic substituent is borne either by the C-2 or N-10 atoms, shows that structural features are also important in determining the relative contributions of stacking and hydrophobic interactions leading to dimerization or micellization.

Results and Discussion

All the kinetic and thermodynamic measurements were carried out in buffered water at pH 7.4. As a preliminary, the protonation of **1b** at this pH was investigated. Spectroscopic measurements show that the absorption spectrum of **1b** remains unchanged between pH 2 and pH 11, with a main band at 305 nm (Fig. S1†). When the pH is increased from 11 to 14, a new band appears at 326 nm and an isosbestic point is observed at 314 nm. These spectroscopic changes were unambiguously attributed to the deprotonation of the N-6 nitrogen atom. The p*K*-value, obtained from the pH dependence of the two bands[7] at 305 and 326 nm, is *ca.* 13.1 ± 0.3 at 25 °C. All the chromophoric molecules studied are, therefore, monocationic species,[7,8] except **2d** which is dicationic, with acetate as the counterion.

Dimerization.—Equilibrium constants for the dimerization of **2a–d** [eqn. (1) where M and D are the monomeric and dimeric species, respectively] were obtained either from spectroscopic measurements (K_d = [D]/[M]^2) and/or relaxation experiments ($K_d = k_1/k_{-1}$).

$$2\,M \underset{k_{-1}}{\overset{k_1}{\rightleftharpoons}} D;\ K_d = [D]/[M]^2 = k_1/k_{-1} \qquad (1)$$

The UV–VIS *spectra* of the chromophoric compounds **2** exhibit two absorption maxima at 313 and 304 nm, as illustrated in Fig. 1(*a*) in which the concentration and temperature-

† Supplementary publication Sup. No. 56942 (6 pp). For details of the supplementary data deposition scheme see 'Instructions for Authors (1993).' *J. Chem. Soc., Perkin Trans. 2*, 1993, issue 1.

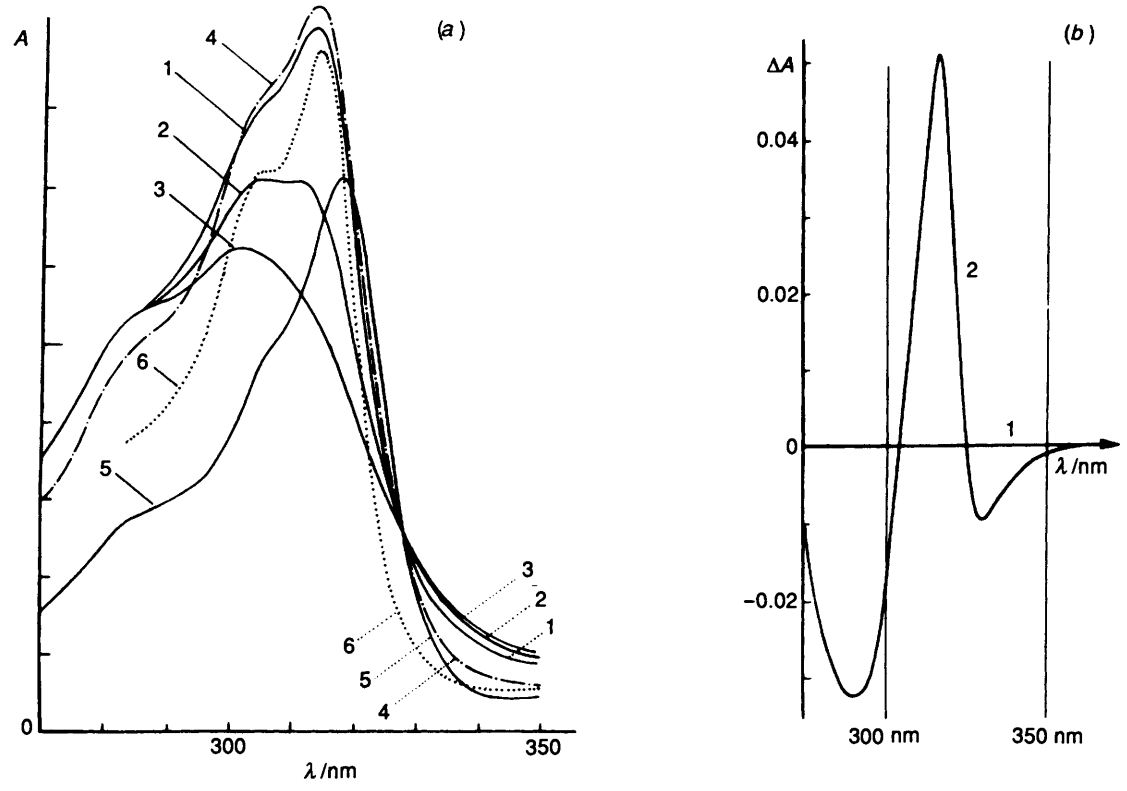

Fig. 1 UV-Absorption spectra of 2-pentyl-OPC, **2b**, and 10-pentyl-OPC, **2c**, in 0.01 mol dm^{-3} aqueous cacodylate buffer pH 7.4. (*a*) Temperature, concentration and solvent dependence: 1, 45 °C: 2, 25 °C and 3, 7 °C for [**2b**] = 3.9 μmol dm^{-3} (0.02 absorb. unit/div): 4, 25 °C for [**2b**] = 2.3 μmol dm^{-3} (0.01 absorb. unit/div): 5. 7 °C for [**2b**] = 23.4 μmol dm^{-3} in unbuffered ethanol (0.2 absorb. unit/div); 6, 25 °C for [**2c**] = 1.8 μmol dm^{-3} (0.01 absorb. unit/div). (*b*) Effect of dilution on the differential absorption spectrum of 10-pentyl-OPC, **2c**, at 25 °C: 1, C_0 = 35 μmol dm^{-3}, l = 2 mm, in both reference and analysis cells; 2, C_0 = 7 μmol dm^{-3}, l = 10 mm, in analysis cell; same conditions as 1 in reference cell. l = optical pathway: C_0 = **2c** analytical concentration).

dependence of the **2d** spectrum are shown. As the concentration increases or temperature decreases, the intensity of the band at 313 nm decreases and becomes smaller than that of the 304 nm band. The observation of an approximate isosbestic point, at about 326 nm, suggests that, at high concentration, a new band occurs at around 330 nm as it appears clearly on the differential absorption spectra [Fig. 1(*b*)]. According to the molecular exciton theory,[9] the excited-state level in the dimer is degenerated, leading to new high and low energy levels. The physical basis of this excited state resonance splitting is related to an electrostatic interaction between transition electric dipoles on neighbouring molecules. Accordingly, the unperturbed 313 nm transition observed in very dilute solutions (or at high temperature and in absolute ethanol) [Fig. 1(*a*), spectrum 5] can be assigned to the monomer (M-band) while the blue-shifted (304 nm; H-band) and the red-shifted (330 nm; J-band) transitions can be attributed to allowed electronic transitions in the dimeric aggregate.[7]

The dimerization constants, K_d, have been obtained from the concentration dependence of the molar absorption coefficients using the Schwarz relationship,[10] eqn. (2); where ε_m and ε_d

$$\sqrt{([\varepsilon_m - \varepsilon]/C_0)} = \sqrt{(2\,K_d/[\varepsilon_m - \varepsilon_d])}\,([\varepsilon_m - \varepsilon_d] - [\varepsilon_m - \varepsilon]) \quad (2)$$

are the molar absorption coefficients of monomer and dimer, ε the apparent molar absorption coefficient at 313 nm (the wavelength corresponding to the absorption maximum of the M-band) and C_0. the total dye concentration. ε_m-Values evaluated according to the procedure described in ref. 10 are 51 000. 45 000. 52 000 and 50 500 dm^3 mol^{-1} cm^{-1} for **2a**, **2b**, **2c** and **2d**. respectively. It is noticeable that ε_m does not depend significantly on the molecular structure, except that of **2b** which is markedly smaller than those of the other compounds.

According to eqn. (2), plots of $\sqrt{[\varepsilon_m - \varepsilon]/C_0}$ *versus* $[\varepsilon_m - \varepsilon]$ give straight lines (Fig. S2) from which K_d values are obtained:[10] 1.8 × 10^5, 2.3 × 10^5, 4.2 × 10^5 and 1.5 × 10^5 dm^3 mol^{-1} for **2a**, **2b**, **2c** and **2d**, respectively.

Kinetic data of the dimerization equilibria (1) have been measured by the T-jump relaxation technique.[11,12] Typical relaxation signals for **2a**, **2b**, **2c** and **2d** solutions are shown in Fig. 2. For all these derivatives, the total amplitude of the relaxation signal depends on the wavelength of the analysis, as do the differential spectra obtained by subtracting the monomer spectrum from the aggregate spectra. This is evidence for the fact that the relaxation processes may be related to the aggregation equilibrium.

The relaxation signals are unambiguously monoexponential for **2a**, **2c** and **2d** but not for **2b**. It is reasonable to assume, therefore, that the unique relaxation time, τ, in the 20–150 μs range, arises from the shift of equilibrium (1), and is related[13] to the rate constants, k_1 and k_{-1}, by eqn. (3).

$$\tau^{-2} = 8\,k_1 k_{-1}[C_0] + (k_{-1})^2 \quad (3)$$

As expected from this equation, the plot of τ^{-2} *versus* C_0, the total dye concentration, is linear (Fig. 3). The intercept, $(k_{-1})^2$, and the slope, $8\,k_1 k_{-1}$, give the kinetic constants (Table 1) from which K_d-values can be calculated. The rate constants of **1a** and **1b** have been also measured, in order to compare their K_d-values with those found for **2** (Table 1). However, the very short relaxation times obtained for large concentrations of **1a** and **1b** are in the same range as the temperature-jump duration. The rate constants deduced from approximate τ-values would therefore be less accurate than those obtained for the OPC series, **2a–d**. Equilibrium constants for dimerization of **1a**, **b** have been measured from the relaxation amplitudes, δS_0 (in mV, see fig. 2), measured at several initial dye concentrations,

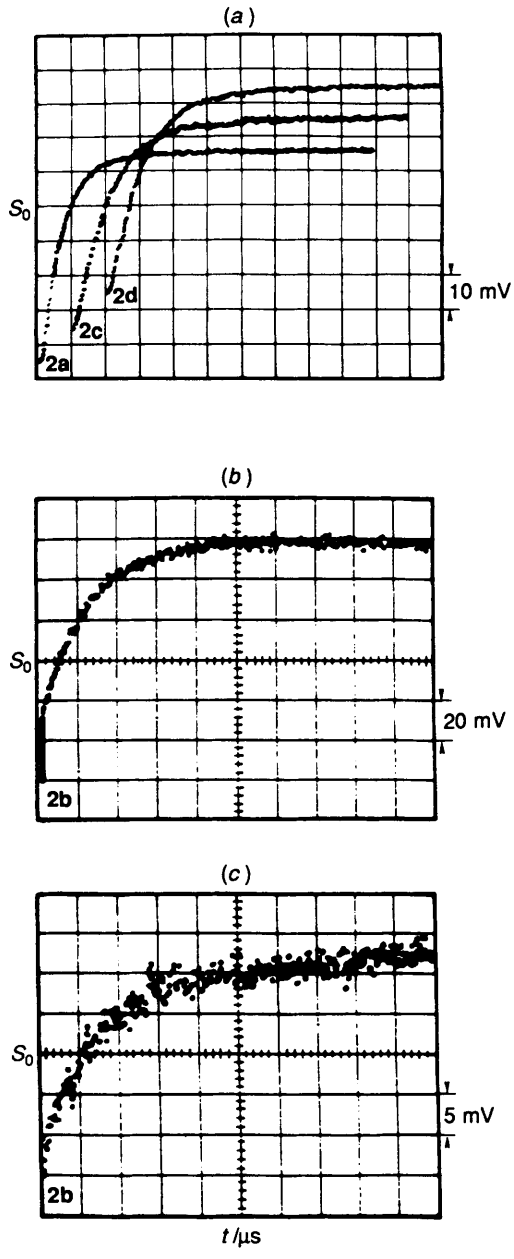

Fig. 2 T-Jump relaxation signals of OPC derivatives in 0.01 mol dm $^{-3}$ cacodylate aqueous buffer pH 7.4. 0.1 mol dm^{-3} NaCl, at 25 °C. Upper: [**2a**] = 2 μmol dm $^{-3}$ 100 μs/div. [**2c**] = 33 μmol dm $^{-3}$, 50 μs/div. [**2d**] = 18.7 μmol dm $^{-3}$. 50 μs/div. Middle: [**2b**] = 31 μmol dm $^{-3}$, 50 ms/div (*slow* phase recording). Lower: [**2b**] = 31 μmol dm^{-3}. 100 μs/div (*fast* phase recording).

All the relaxation curves correspond to an increase in the absorbance of the solution.

C_0, using relationship (4) where $C_{0.max}$ is the C_0-value at the maximum of the plot $\delta S_0/c_0$ *versus* C_0,[12] as shown in Fig. 4.

$$k_d\, C_{0.max} = 0.603 \qquad (4)$$

All the thermodynamic and kinetic results are collected in Table 1. There is a satisfactory agreement between the K_d-values obtained either from the UV spectra or in relaxation experiments. The fact that the values from kinetics are somewhat larger than those from spectroscopic studies probably arises from the large ionic strength (0.11 mol dm $^{-3}$) used in the relaxation technique and which may favour stacking because of screening of the positive charges by the salt anions.[4] This fair agreement supports the initial assumption that ellipticinium

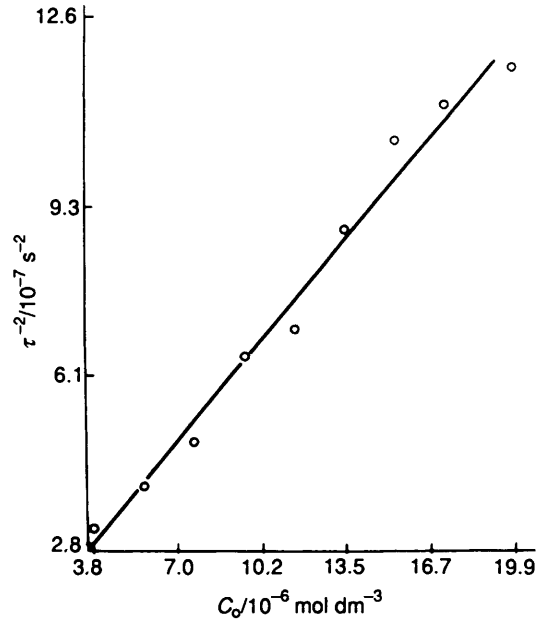

Fig. 3 Determination of the rate constants for the 10-pentyl-OPC dimerization from the plot of τ^{-2} *versus* [**2c**] in 0.01 mol dm $^{-3}$ cacodylate buffer pH 7.4, 0.1 mol dm $^{-3}$ NaCl at 25 °C, according to eqn. (3)

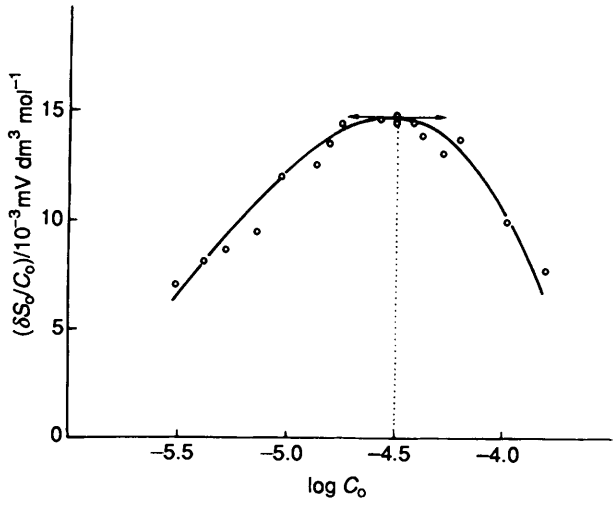

Fig. 4 Determination of the dimerization constant for 2-NME in 0.01 mol dm $^{-3}$ cacodylate aqueous buffer pH 7.4, 0.1 mol dm $^{-3}$ NaCl at 25 °C, according to eqn. (4)

derivatives autoaggregate *via* a dimerization mechanism. However, substitution at the C-2 carbon atom of the polycyclic OPC with a pentyl group modifies this mechanism since the behaviour of **2b** in relaxation experiments differs from those of the other derivatives.

K_d-Values for ellipticinum and its *N*-methyl analogue, **1a** and **1b**, are noticeably smaller than those of compounds **2**. The increase in K_d on going from **1** to **2** probably arises from the increase in London-type dispersion interactions arising from the extension of the π-electron aromatic system by adding the oxazole ring. The hydrophobic character of the methyl substituent can explain the K_d increase observed between **1a** and **1b**.

Inspection of Table 1 also reveals that the dimer stability depends on the position of the alkyl substituent on **2a**. Comparison of K_d for **2a** and **2c** shows that the superimposition of stacking and hydrophobic interactions significantly increases K_d. This has already been observed[6] in the 10-alkyl acridine orange series where the nitrogen atom is quaternarized with an aliphatic amino group. Moreover. when there is a charged

Table 1 Kinetic and dimerization constants[a] for self-stacking process of ellipticine derivatives at 25 °C in aqueous media

	k_1/ 10^8 dm^3 mol^{-1} s^{-1}	k_{-1}/ 10^3 s^{-1}	K_d/10^5 dm^3 mol^{-1}			ε_m/10^4 dm^3 mol^{-1} cm^{-1}[e]
			b	*c*	*d*	
1a	2.4	49	0.049	0.076[f]		
1b	6.4	27	0.24	0.19		
2a	10.2	6.6	1.5	1.7	1.4	5.10
2b					2.3	4.50
2d	3.6	2.1	1.7		1.5	5.05
2c	8.5	1.9	4.5		4.2	5.20

[a] In 0.01 mol dm^{-3} cacodylate buffer. pH 7.4, 0.1 mol dm^{-3} NaCl. [b] From k_1/k_{-1}. [c] From the amplitude of relaxation signals according to eqn. (4). [d] From spectroscopic measurement according to eqn. (2), without NaCl added. [e] At 313 nm. [f] In 0.1 mol dm^{-3} acetate–acetic acid. buffer pH 5.

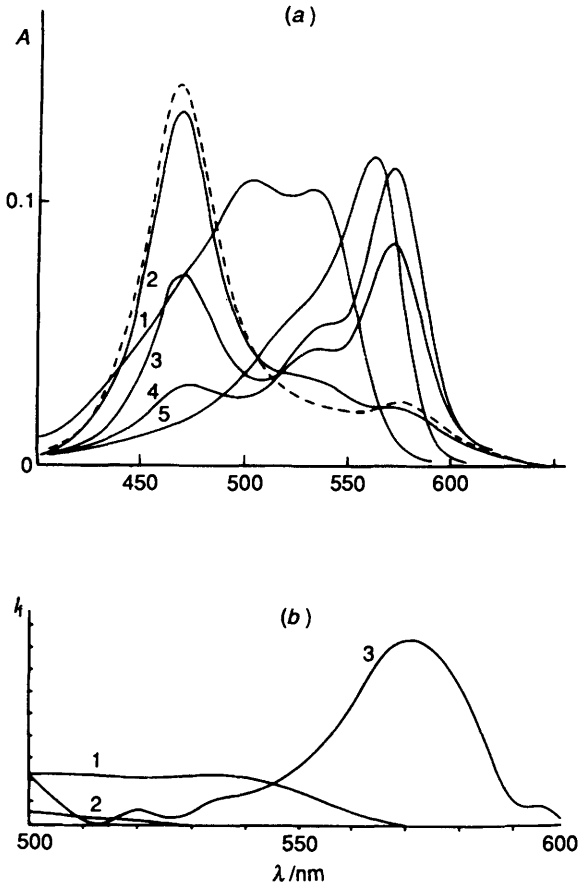

Fig. 5 Effects of the addition of ellipticinium derivatives on MC540 spectra (0.01 mol dm^{-3} cacodylate aqueous buffer pH 7.4, 0.1 mol dm^{-3} NaCl at 25 °C). (*a*) Visible absorption spectra of MC540 (2 μmol dm^{-3}) in the presence of 2-pentyl-OPC. **2b**, 10-pentyl-OPC, **2c**, and CTABr micelles: 1, [**2b**] = 0 μmol dm^{-3}: 2, [**2b**] = 11.6 μmol dm^{-3}; 3, [**2b**] = 27.1 μmol dm^{-3}; 4, [**2b**] = 54.1 μmol dm^{-3}: 5, micellar [CTABr] = 2.3 10^{-3} mol dm^{-3}: dashed curve: [**2c**] = 2.3 μmol dm^{-3}. (*b*) Fluorescence excitation spectra at 600 nm: 1, [MC540] = 7.7 μmol dm^{-3}; 2, [**2b**] = 54.1 μmol dm^{-3}: 3, 1 + 2.

hydrophilic amino group in terminal position, **2d**, a lower K_d-value, similar to that of the unsubstituted **2a**, is obtained, as a direct consequence of a hydrophobicity loss equivalent to four methylene units.

As shown in Table 1, all the rate constants of the dimer formation, k_1, are in the range 10^8–10^9 dm^3 mol^{-1} s^{-1}, which is typical of a diffusion-controlled process involving solvated, bulky species.[14] A significant rate increase, parallel to that observed for K_d, is found on going from **1a** to **1b** and **2a**. The k_1-value for **2d**, which is smaller than those found for the other OPC derivatives, may be ascribed to the occurrence of hydrophilic interactions between the charged NH_3^+ substituent and the bulk water. In contrast, the reverse rate constants, k_{-1}, decrease markedly in the order **1a** < **1b** < **2**. Combination of the increase in k_1 and decrease in k_{-1} leads to an important increase in the K_d-values on going from **1a** to **1b** and to **2**. It appears, therefore, that the stability of the ellipticinium dimers is mainly controlled by their breakdown rates.

Micellization of 2-Pentyl-OPC, **2b**.—Since the relaxation signal of **2b** is not mono- but bi-exponential, its self-association mechanism cannot be as simple as dimerization. We investigated, therefore, micellization, another possible aggregation mechanism. Changes in absorption and fluorescence spectra of merocyanine 540 (MC540) observed in the presence of organized hydrophobic structures have been used to probe micelle formation in solution.[15] This highly sensitive method is useful for detecting micellization using only a few micrograms of an amphiphilic compound. The absorption spectrum of a 2 μmol dm^{-3} MC540 aqueous solution [Fig. 5(*a*)] shows two maxima at 501 and 534 nm, which have been previously attributed to contributions from both dimeric and monomeric structures of the dye.[12] When increasing amounts of **2a–d** are added to the aqueous dye in the presence of 0.1 mol dm^{-3} NaCl, a new absorption band appears at about 470 nm with an isosbestic point at 518 nm. In the particular case of **2b**, further drug addition (≥ 15 μmol dm^{-3}; 0.1 mol dm^{-3} NaCl) leads to a new red-shifted band at 572 nm, which is characteristic of MC540 interaction with SDS anionic[13] or CTABr cationic micelles [spectrum 5, Fig. 5(*a*)]. In the presence of large concentrations of **2b** (up to 2×10^{-5} mol dm^{-3}), the fluorescence excitation spectrum of MC540 displays a red shift from *ca.* 535 nm to *ca.* 570 nm, associated with a large increase in the fluorescence intensity [Fig. 5(*b*)]. These spectroscopic effects are not observed in the presence of **2a**, **2c** and **2d**. These absorption and fluorescence spectroscopic changes suggest that, in the concentration range studied, only **2b** shows micellar behaviour when the ionic strength of the solution is maintained at 0.1 mol dm^{-3}, under similar conditions used in relaxation experiments. A plot of the fluorescence intensity (λ_{em} = 610 nm, λ_{exc} = 565 nm) *versus* [**2b**] [Fig. 6(*a*)], therefore, used[15] to determine its critical micellar concentration (cmc), which is found to be 1.9×10^{-5} mol dm^{-3} in 0.1 mol dm^{-3} NaCl, at 25 °C. It is important to mention that when MC540 experiments are carried out in the absence of any added salt, *i.e.*, under concentration conditions similar to those used in UV experiments from which dimerization constants have been obtained, **2b** behaves as the other compounds **2**. Therefore, there is no evidence for **2b**-micellization in the absence of added salt.

Evidence for the micellization of **2b** at high ionic strength is also found from the **2b** fluorescence spectrum. As shown in Fig. 6(*b*), the concentration dependence of the fluorescence intensity at 530 nm (λ_{exc} = 305 nm) is not linear over the total concentration range. Two kinds of behaviour are observed. At very small **2b** concentrations ([**2b**] < 5×10^{-7} mol dm^{-3}), where it is reasonable to assume that **2b** is in its monomeric form

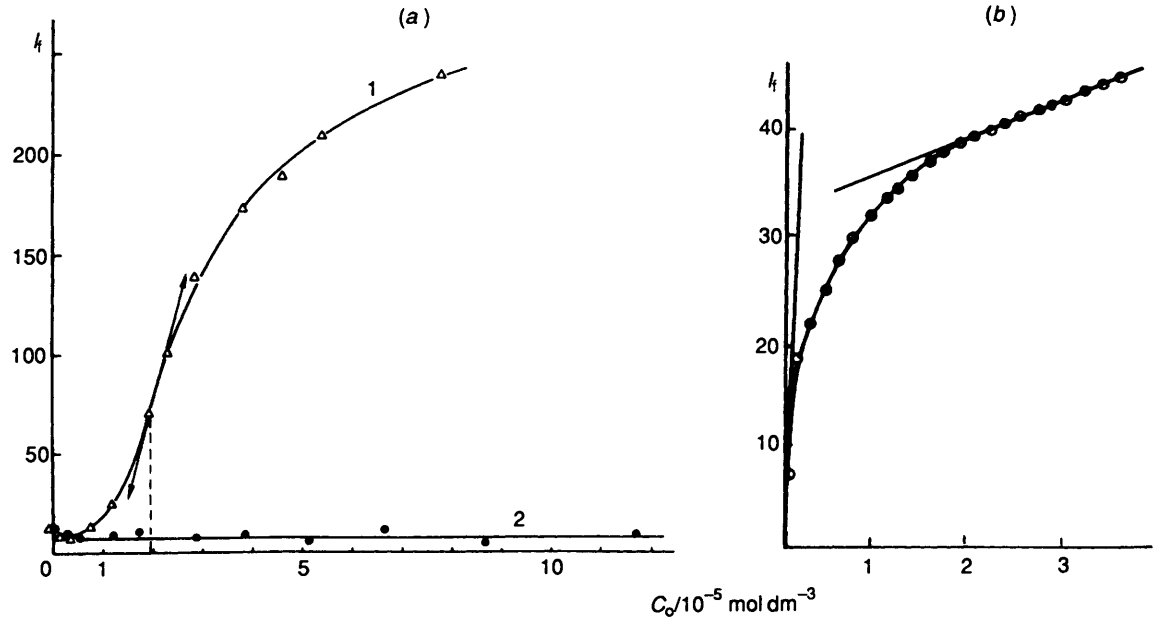

Fig. 6 Determination of the critical micellar concentration (cmc) of 2-pentyl-OPC, **2b**, at 25 °C (0.01 mol dm^{-3} cacodylate aqueous buffer pH 7.4. 0.1 mol dm^{-3} NaCl). (*a*) Plot of I_f at 600 nm *versus* [OPC] with MC540 probe (7.7 μm), λ_{exc} = 565 nm. 1, **2b**; 2, **2d** or **2c**. (*b*) Plot of I_f at 530 nm *versus* [**2b**]. λ_{exc} = 305 nm.

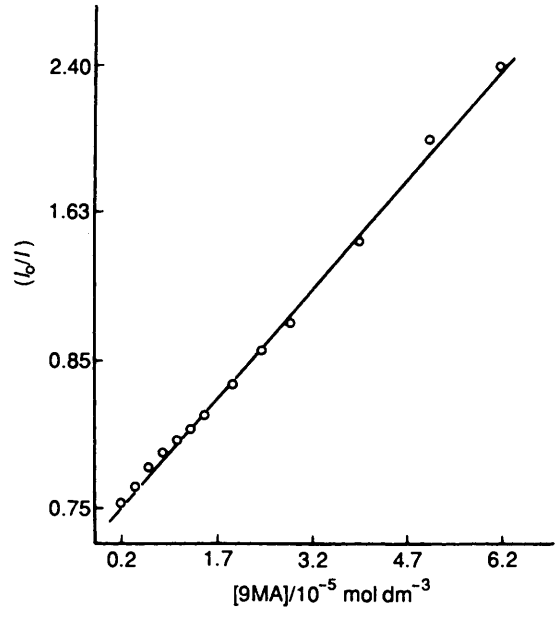

Fig. 7 9MA quencher concentration dependence of DPH fluorescence intensity at 25 °C. according to eqn. (5). [**2b**] and [DPH], 3.86 × 10^{-4} and 4 × 10^{-6} mol dm^{-3}. respectively: [9-MA] and [DPH] = 9-methylanthracene and diphenylhexatriene concentrations: λ_{exc} = 338 nm. λ_{em} = 480 nm.

only, the expected linearity of the I_f *vs.* [**2b**] plot is found. At high concentrations ([**2b**] > 2 × 10^{-5} mol dm^{-3}) where micellization is the most likely, linear behaviour is also observed but with a slope about ten times smaller. From this concentration dependence of the fluorescence intensity, an approximate cmc-value, in the 2 × 10^{-5} mol dm^{-3} range, can be estimated, in fair agreement with that obtained with the MC540 probe.

The mean aggregation number (N_{ag}) of **2b** micelles has been measured by the procedure[16] which consists of quenching of a luminescent probe by a known amount of a quencher. This method is particularly suitable for the determination of N_{ag} using very small amounts of surfactant. In the following experiments. diphenylhexatriene (DPH) and 9-methylanthracene (9MA) have been used as the fluorescent probe bound to the **2b** micelles and as the quencher, respectively. The mean aggregation number N_{ag} is obtained from eqn. (5), where I_0 and I are the fluorescence intensities of DPH in the absence and in

$$\ln (I_0/I) = N_{ag}[9MA]/([\mathbf{2b}] - \text{cmc}) \quad (5)$$

the presence of 9MA, respectively. [**2b**] is the analytical drug concentration and cmc is the critical micellar concentration. This equation predicts a linear variation of ln (I_0/I) with [9MA], as is found experimentally (Fig. 7). With 2 × 10^{-5} mol dm^{-3} for the cmc-value, the slope of this straight line gives an estimation of N_{ag} corresponding to 15 monomers per micelle.

The parameters of the MC540 binding to **2b** micelles were also measured in titration experiments of a **2b** solution (0.1 mol dm^{-3} NaCl) by increasing the amounts of MC540. The Scatchard isotherm[17] was used to analyse the experimental data. The slope and the intercept on the *x*-axis of the titration curve (Fig. S3) give the affinity constant, K_a = 10^6 dm^3 mol^{-1}, and the maximum number of MC540 molecules bound to one **2b** molecule, n = 0.09, *i.e.*, one MC540 for every ten **2b** monomers.

In the particular case of 2-pentyl-OPC solutions at concentrations larger than 2 × 10^{-5} mol dm^{-3}, two relaxation times, in very different time scales (10–100 μs for the faster, 5–350 ms for the slower) are observed (Fig. 2, **2b**), when the ionic strength is 0.11 mol dm^{-3}. This suggests the involvement of, at least, a two-step mechanism as previously described for micellization processes[18] [eqn. (6)].

$$(n+1)\,\mathrm{M} \underset{k_2}{\overset{k_2}{\rightleftharpoons}} \mathrm{M}_n + \mathrm{M} \underset{k_1}{\overset{k_1}{\rightleftharpoons}} \mathrm{M}_{n+1} \quad (6)$$

(slow step, τ_2) (fast step, τ_1)

In this mechanism, the fast relaxation arises from the exchange of one monomer M between M_{n+1} and M_n micelles and the slow one, from the micellization–dissolution equilibrium. The concentration dependence of the fast relaxation time is given[18] by eqn. (7) in which σ represents the width of

$$1/\tau_1 = (k_1/\sigma^2) + (k_1/N_{ag})(C_0 - \text{cmc})/\text{cmc} \quad (7)$$

the distribution curve of micelles. According to eqn. (7). a plot of τ_1^{-1} *versus* C_0 (Fig. 8), gives a straight line whereas the

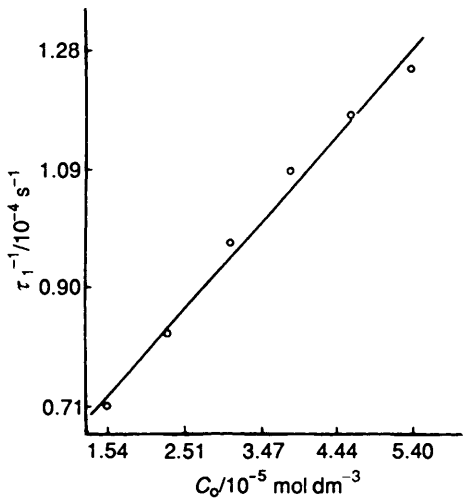

Fig. 8 Plot of the reciprocical fast relaxation time τ_1^{-1} *versus* 2-pentyl-OPC concentration according to eqn. (7). at 25 °C

Table 2 Parameters of 2-pentyl-OPC micellization at 25 °C[a]

(N_{ag}/k_1)/μs	380
(k_1/σ^2)/s^{-1}	7500
N_{ag}	15
σ	3
cmc/mol dm^{-3}	2×10^{-5}
k_1/s^{-1}	3.9×10^4
k_2/dm^3 mol^{-1} s^{-1}[b]	2.0×10^9

[a] In 0.01 mol dm^{-3} cacodylate buffer. pH 7.4, 0.1 mol dm^{-3} NaCl. [b] Obtained using the equation[19] $k_2 = k_1$/cmc.

analogous plot of τ_2^{-1} is curved (Fig. S4), as has been previously observed for various ionic surfactants.[19] From the linear behaviour of τ_1^{-1}, the residence time of one **2b** monomer in the micelle, N_{ag}/k_{-1}, can be estimated to be *ca.* 380 μs.

All the parameters measured for micellization of **2b** at concentrations higher than 2×10^{-5} mol dm^{-3} and at 0.1 mol dm^{-3} ionic strength are shown in Table 2. A cmc-value among the smallest presently known is associated with a very small aggregation number whereas, for usual short-chain surfactants, N_{ag}-values in the 20 range correspond to very high cmc values.[19] As regards its cmc, **2b** resembles either a non-ionic or a very long chain ($> C_{16}$) ionic surfactant. The fact that the counterion of **2b** is the hydrophilic acetate may contribute to these small aggregation parameters since it is well known that an increase in the counterion hydration decreases cmc- and N_{ag}-values, significantly. However, in the case of **2b**, an acetate–chloride exchange cannot be excluded since micellization is observed in the presence of high sodium chloride concentration. It must also be pointed out that the literature data concerning micellization processes have generally been obtained without any added salt, the influence of which is far from understood.

In this respect, it is interesting to note that, when MC540 experiments are carried out in the absence of chloride ions, no evidence for micellization is found in the very small **2b** concentration range. However, when **2b** concentration becomes as high as 4×10^{-3} mol dm^{-3} (the highest we can obtain), a significant increase in the intensity of the fluorescence emission at 600 nm (λ_{exc} = 565 nm), characteristic of micellization, appears.

It is possible, therefore, that **2b** micellizes even in the absence of salt. but with a cmc-value in the usual 10^{-3}–10^{-2} mol dm^{-3} range.

In contrast. dynamic results are more similar to those usually found for classical surfactants.[19] The residence time. 380 μs, and micellization rate, 2×10^9 dm^3 mol^{-1} s^{-1}, are in the usual range for cationic micelles. The exchange between monomers and micelle, $k_{-1} = 3.9 \times 10^4$ s^{-1}, is rather slow, but not exceedingly so, as compared with those measured for long-chain surfactants. Apart from the mean aggregation number, **2b** more closely resembles C-16 ionic surfactants. This unexpected behaviour probably comes from the specific structural features of **2b**, where a shorter pentyl chain is associated with a hydrophobic polar head from which stacking interactions, charge delocalization and steric constraints can cooperate to give the aggregation mechanism. Also relevant to the aggregation mechanism of **2b** is the fact that, at small ($> 3 \times 10^{-5}$ mol dm^{-3}) concentration and in the absence of added salt, the K_d-value measured from UV absorption spectra [Table 1, Fig. 1(*a*)] corresponds fairly well with a dimerization process similar to that evidenced for the other compounds **2**.

Conclusions

A number of structural requirements for micellization are suggested from comparisons of **2b**, **2c** and **2d** which all involve a pentyl chain. When the hydrophobic character of this short chain is, at least in part, eliminated by the terminal NH_3^+ group, as in **2d**, there is no micellization and stacking interactions promoting dimerization prevail. Since **2c**, in which the two hydrophobic groups are branched on the cationic head, does not micellize either, the pentyl chain and the polyaromatic chromophore cannot adopt a conformation suitable for minimizing their interactions with water. In other words, in **2c**, there is no additivity, or cooperativity, of the group hydrophobicities and again stacking interactions prevail. In the case of **2b** only, which is the unique amphiphilic molecule of the series, the pentyl chain probably provides a significant increase in the chromophore hydrophobicity and micellization does occur, *i.e.*, hydrophobic interactions are large enough to overcome the stacking effects.

More work is in progress to understand better the subtle balance between the stacking and hydrophobicity which determine the energetically favoured aggregation mechanism, dimerization or micellization.

Experimental

Chemicals.—Ellipticine base (E) and 2-methylellipticinium (2-NME) were generous gifts from Dr. E. Lescot (IGR, Villejuif, France).

9-Hydroxy-2-pentylellipticine was synthesized by reaction of 1-bromopentane with 9-hydroxyellipticine at 60 °C under reflux overnight and separated by chromatography on a silica column in 5:1 acetic acid–methanol.

H-OPC (7,10,12-trimethyl-6*H*-oxazolo[4,5-*a*]pyrido[4,3-*i*]-carbazolium acetate), 2-pentyl-OPC, 2-aminopentyl-OPC and 10-pentyl-OPC were synthesized according to previously published procedures.[2,3] H-OPC, 2-pentyl-OPC, 2-amino-pentyl-OPC were obtained from enzymatic oxidation (H_2O_2–horseradish peroxidase system) of 9-hydroxy-2-methylellipticine followed by either glycine, pentylamine or pentane-1,5-diamine nucleophilic addition at C-10. 10-Pentyl-OPC was similarly obtained by addition of glycine 9-hydroxy-2-pentylellipticine.

Aliphatic-OPCs were purified by reversed-phase chromatography using a hydrophobic XAD2 column and ammonium acetate buffer–methanol gradients as the eluent. The purity of each compound was checked by high performance liquid chromatography and thin layer chromatography. Mass spectra were recorded on a VG 70-250 double focusing magnetic instrument (VG analytical, UK) equipped with a fast atom

bombardment gun (Ion Teck, UK) operated at 6 kV. Scans were obtained at 10 s decade^{-1} with an interscan time of 2 s. Glycerol and thioglycerol were used as both matrix and internal standard.

Merocyanine 540 (MC540) was purchased from Eastman Kodak, diphenylhexatriene (DPH) from Aldrich, 9-methylanthracene (9MA) and *n*-hexadecyl(trimethyl)ammonium bromide (CTABr) from Jansen Chemica. MC540, DPH and 9MA were used without further purification. CTABr was purified by successive recrystallization from ethanol–water mixtures before use.[20]

The standard aqueous buffer used in spectroscopic measurements was 0.01 mol dm^{-3} cacodylic acid–sodium cacodylate, pH 7.40. For T-jump relaxation kinetics, 0.1 mol dm^{-3} NaCl was added to this buffer in order to speed up the Joule temperature rise, so that the ionic strength was 0.11 mol dm^{-3}.

Spectroscopy.—Spectra recordings and spectroscopic determinations of the dimerization constants of OPCs were performed, in 3 cm^3 quartz cells, using a Cary 118 spectrophotometer equipped with a thermostatted cell holder. The temperature was controlled to within ±0.5 °C using a UK20 cryostat (Lauda).

Fluorescence experiments were performed on a Perkin-Elmer LS-5 luminescence spectrophotometer. Differential spectra were recorded using two quartz cells of 1 cm and 0.2 cm optical pathways, thus allowing the determination of the non-linear contributions to the concentration dependence of the absorbance.[12]

Since micelle formation is not a thermodynamic transition occurring at a rigorously defined surfactant concentration and since it spans an extended concentration range, the cmc of 2-pentyl-OPC was arbitrarily taken at the inflection point of the curve[15] shown in Fig. 6(*a*).

The MC540 binding constant to **2b** micelles, K_a, was determined from fluorescence titration experiments taking advantage of the high fluorescence emission of the bound MC540. The excitation and emission wavelengths leading to the optimal differences in fluorescence intensity between free and bound MC540, were found at 565 nm and 600 nm, respectively.

The concentration of MC540 bound to OPC micelles, C_b, was calculated according to eqn. (8) where δI_f is the difference in

$$C_b = \delta I_f/[K(V - 1)] \quad (8)$$

fluorescence intensity between free and bound MC540, K a factor relating free MC540 concentration ($[MC540]_{free}$) to the fluorescence intensity and V, the relative fluorescence quantum yield of bound and free MC540. V was estimated from the double reciprocical plot of I_f *versus* OPC concentration. Values of r (the ratio of bound MC540 to the total OPC concentrations) and L ($L = [MC540]_{free}$), obtained from binding experiments, were analysed according to the Scatchard equation[17] $r/L = K_a(n - r)$.

Kinetic Experiments.—Kinetics of aggregation equilibria were performed using a Messanlagen Studengesellschaft Joule-heating T-jump spectrometer.[12] At 0.11 mol dm^{-3} ionic strength, a 5 °C temperature jump was obtained within 5 μs by discharging a 0.05 μF capacitor charged to 20 kV across a 2 cm^3 cell. All experiments were performed at 20 °C so that the final temperature was 25 °C. Analysis wavelengths were selected either at 313 nm (OPCs, E) or at 305 nm (2-NME). Since drugs show low photostability, the intense UV light from the analysis beam was cut between each T-jump run. Relaxation signal recordings were transferred to a PDP11 computer *via* a high-speed digital interface. Three relaxation curves were summed and analysed by least-squares fitting procedures. The amplitude measurements were performed by direct reading from a Tecktronic R 7912 oscilloscope screen after a 20 kV discharge voltage. Accuracy on the relaxation times and amplitudes was estimated to be ±10% and ±5%, respectively.

References

1 N. Nagasawa, M. Homma, H. Namiti and K. Niki, *Eur. J. Cancer Clin. Oncol.*, 1984, **20**, 273; C. L. Artega, D. L. Kiesner, A. Goodman, D. D. Von Hoff, *Eur. J. Cancer Clin. Oncol.*, 1987, **23**, 1621.
2 C. Auclair, E. Voisin, H. Banoun, C. Paoletti and B. Meunier, *J. Med. Chem.*, 1984, **27**, 1161; C. Auclair, M. A. Schwaller, B. René, H. Banoun, J. M. Saucier and A. K. Larsen, *Anti-Cancer Drug Design*, 1988, **3**, 133.
3 R. Sundaramoorthi, K. V. Kansal, B. C. Das and P. Potier, *J. Chem. Soc., Chem. Commun.*, 1986, **371**, 1645; A. Gouyette, C. Auclair and C. Paoletti, *Biochem. Biophys. Res. Commun.*, 1985, **131**, 614.
4 H. Porumb, *Prog. Biophys. Mol. Biol.*, 1978, **34**, 175.
5 G. S. Levinson, W. T. Simpson and W. Curtiss, *J. Am. Chem. Soc.*, 1957, **79**, 4314.
6 L. Constantino, O. Ortena, R. Sartorio, L. Sylvestri and V. Itagliano, *Adv. Mol. Relax. Interact. Proc.*, 1981, **20**, 191; M. Septinus, W. Seiffert and H. W. Zimmermann, *Histochemistry*, 1983, **79**, 443; K. Murakami, K. Mizuguchi, Y. Kubota and Y. Fugisaki, *Bull. Chem. Soc. Jpn.*, 1986, **59**, 3393.
7 A. Adenier, J. Aubard and M. A. Schwaller, *J. Phys. Chem.*, 1992, in press.
8 G. Dodin, M. A. Schwaller, J. Aubard and C. Paoletti, *Eur. J. Biochem.*, 1988, **176**, 371.
9 M. Kasha, H. R. Rawls and M. Ashraf El Bayoumi, *Pure Appl. Chem.*, 1965, **11**, 371.
10 G. Schwarz, S. Klose and W. Balthasar, *Eur. J. Biochem.*, 1970, **12**, 454.
11 T. G. Dewey, D. Raymond and D. H. Turner, *J. Am. Chem. Soc.*, 1979, **12**, 5822.
12 A. Adenier and J. Aubard, *J. Chim. Phys.*, 1987, **84**, 921.
13 C. F. Bernasconi, *Relaxation Kinetics*, Academic Press, New York, 1976.
14 M. A. Schwaller, G. Dodin and J. Aubard, *Biopolymers*, 1991, **31**, 519.
15 G. Dodin, J. Aubard and D. Falque, *J. Phys. Chem.*, 1987, **91**, 1166.
16 N. J. Turro and A. Yekta, *J. Am. Chem. Soc.*, 1978, **18**, 5951; F. Grieser and C. J. Drummond, *J. Phys. Chem.*, 1988, **92**, 5580.
17 G. Scatchard, *Ann NY Acad. Sci.*, 1949, **51**, 660.
18 J. Lang, C. Tondre, R. Zana, R. Bauer, H. Hoffmann and W. Ulbricht, *J. Phys. Chem.*, 1975, **79**, 276.
19 E. A. G. Anianson, S. N. Wall, M. Almgren, H. Hoffmann, I. Kielmann, W. R. Ulbricht, R. Zana, J. Lang and C. Tondre, *J. Phys. Chem.*, 1976, **80**, 905.
20 A. Berthod, I. Girard and C. Gonnet, *Anal. Chem.*, 1986, **58**, 1362.

Paper 2/06308E
Received 25*th November* 1992
Accepted 15*th February* 1993